*(Submitted in October of 2005 to review for the 8th U.S. National Conference on Earthquake Engineering.)*

# EFFECTS OF RUPTURE DIRECTIVITY ON EARTHQUAKE LOSS ESTIMATION

By Paolo Bazzurro[1], Brian Sjoberg[2], Jaesung Park[2], and Nicolas Luco[3]

## ABSTRACT

A seismic loss estimation analysis, whether for a single structure or a portfolio of properties, requires a relationship between a chosen ground motion intensity measure, IM, and economic loss. This relationship, called a Loss Function, LF, is developed here by a two-step procedure that combines *analytical* and *empirical* data. First an analytical relationship is built via engineering analyses performed on a mathematical model of a structure, and then the resulting function is calibrated using loss data from past earthquakes. One key aspect of developing the analytical function is to create a "link" between one (or more) IM(s) and one (or more) measure(s) of the demand that the ground motion imposes on the structure. This link is often established using regression analysis techniques. Typically, the spectral acceleration, $S_a$, at the structure's fundamental period of vibration, $T_1$, is used as the single IM of choice. Studies have shown, however, that near-source, forward-directivity ground motions are, on average, more damaging than other accelerograms with the same $S_a(T_1)$. As intuition suggests, this is true for moderate-to-long period structures that are dynamically driven by the velocity pulses often observed in fault-normal components of forward-directivity records. This study illustrates that this can also be the case for some stiffer structures whose $T_1$ values are significantly shorter than the period of those velocity pulses. We show the impact of this finding in a loss estimation analysis for residential woodframe structures located at single sites and in a portfolio in the San Francisco Bay Area.

## Introduction

Probabilistic loss estimation analyses for natural events such as earthquakes, hurricanes, tornadoes and the like are nowadays routinely performed for a variety of stakeholders. Property owners, insurance and reinsurance companies, capital lending institutions, local government agencies, and structural engineers all have interests, albeit different, in knowing the likelihood that a specific single structure, a category of similar structures, or a portfolio of properties may suffer certain levels of damage and economic losses. Owners and corporate risk managers may use such information to select among risk mitigation strategies that may vary from self-insurance programs (expense funds for post-earthquake recovery, for example, or proactive seismic retrofit) to buying earthquake insurance coverage. Insurance and reinsurance companies may

---

[1] Manager Engineering Analysis, AIR Worldwide, 388 Market Street, Suite 750, San Francisco, CA 94111
[2] Analysis Engineer, AIR Worldwide, 388 Market Street, Suite 750, San Francisco, CA 94111
[3] Senior Project Engineer, AIR Worldwide, 388 Market Street, Suite 750, San Francisco, CA 94111 (Now at United States Geological Survey, Golden, CO)

utilize these risk estimates to set adequate coverage premiums, whereas lending institutions may employ them to decide whether to grant a loan and, if so, at what rate. Local government agencies may look at these findings to decide if certain types of buildings meet current safety standards, and if not whether retrofit measures should be encouraged or mandated. Finally, structural engineers that embrace the vision of performance-based engineering (e.g., see the Pacific Earthquake Engineering Research Center website http://peer.berkeley.edu/ for details) find in these results the necessary background to guide the design or the assessment of structures that are intended to perform according to explicit goals.

In this study, we will focus on an aspect of damage and loss estimation that can be of interest to many such stakeholders. We will look into the vulnerability of stiff, woodframe structures such as those that comprise the overwhelming majority of the residential building inventory in California. In the U.S., the ratio of woodframe structures to total structures is between 80% and 90% (Reitherman and Cobeen, 2003). In particular, we will address the issue of the vulnerability of buildings close to an earthquake fault, as is common in the San Francisco Bay Area and in the Greater Los Angeles region. For example, about two and a half million people live in such houses in the East San Francisco Bay Area in the immediate vicinity of the Hayward Fault, which last generated a large event about 140 years ago and has a 27% chance of generating a large event in the next 30 years (http://quake.wr.usgs.gov/research/seismology/wg02/).

## Development of Loss Functions for Earthquake Loss Estimation Analyses

Regardless of the purpose of an earthquake damage and loss estimation analysis, there is a need for linking the severity of the ground motion with the severity of the physical damage suffered by structures and, ultimately, with the economic losses. The probabilistic relationship that maps the intensity of the ground motion into the economic loss is sometimes called a Loss Function, LF. Ideally one could mine data from past earthquakes and use statistical regression techniques to develop (for many building types) relationships for predicting damage and losses from future temblors. Unfortunately, unlike in other countries (e.g., Italy), the existing damage data in the U.S. are scarce, heterogeneously collected, and statistically biased towards heavily damaged structures. Loss data are, relatively speaking, more plentiful, but are still plagued by the same difficulties mentioned above and, most importantly, are often proprietary in nature. The result is that statistically sound relationships between ground motion parameters and economic losses cannot be obtained for all the desired building categories using historical data alone.

To overcome this partial impasse, the purely empirical approach described above can be replaced by a two-step procedure that combines *analytical* and *empirical* data. For a given structure or class of structures with certain characteristics, first a computer model is built and shaken with a suite of ground motions of different intensity. For each ground motion, first the response of the structure is evaluated. Then the physical damage of each component and the related repair (or replacement) cost to restore its functionality to pre-earthquake conditions are estimated using a Monte Carlo simulation technique. The total loss caused by each ground motion is found by summing the repair or replacement costs for all damaged components. An analytical LF can be derived by regressing the total building losses from all the earthquake records with respect to an appropriate intensity parameter of the ground motions utilized to shake the buildings. This is conceptually the same methodology followed by CUREE (Porter *et al.*, 2002). The derived analytically-based LFs, however, are not usually utilized "as is" in loss estimation analyses, but instead are calibrated using empirical loss data. The relative differences in vulnerability due to variations of the engineering features identified in the analytical study are statistically preserved during this calibration process. Later in this article, we will show a set of analytical LFs for various woodframe buildings. The LFs obtained after the calibration, however, are not presented here due to the proprietary nature of the final loss functions.

## Effects of Rupture Directivity on Stiff Structures

In the earth science and engineering communities it is widely accepted that the characteristics of ground shaking close to a fault rupture generally depend on whether the rupture moves towards the building site or away from it. These two cases are often referred to as *forward directivity* and *backward directivity* conditions, respectively. In the forward directivity case, the horizontal fault-normal component of the ground motion tends to have a one- or two-lobe pulse that is often very apparent in the velocity time histories (e.g., see Fig. 1, Panel a). The average period of such pulses, which appears to be magnitude-dependent (Somerville, 2003), may vary from about 1.5s for a M6.5 event to more than 3s for a M7.5 earthquake. These moderate-to-long period pulses have been recognized to generate, on average, systematically larger responses in moderate-to-long period structures (i.e., those with fundamental period of vibration, $T_1$, longer than 0.5s), as compared to the responses induced by more typical, "rumbling" ground motions of similar severity (e.g., see Fig. 1, Panel b). The latter ground motions are more common both at sites that are located close to the causative fault but in the backward directivity region and at sites that are far away (e.g., 50km or more) from the rupture. It should be recognized, however, that non-pulse-like records have been recorded in the forward directivity region as well.

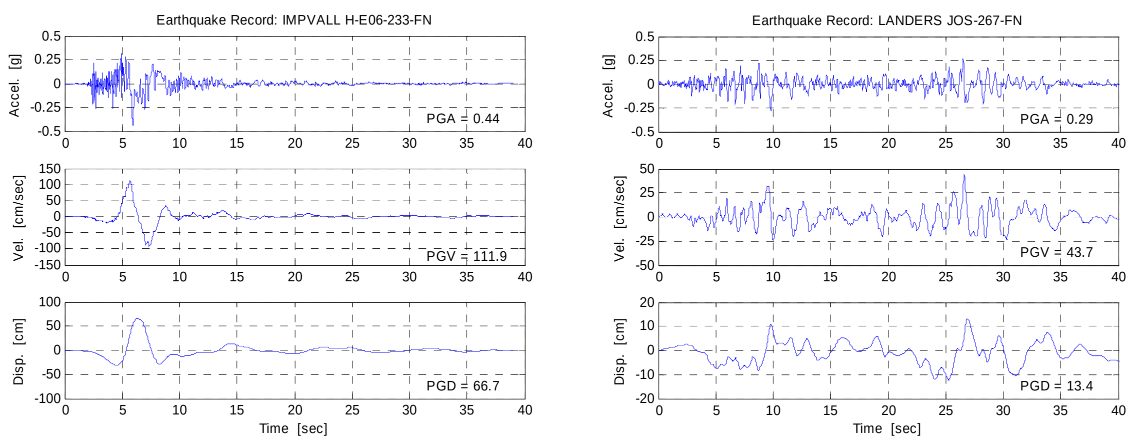


**Figure 1**: Acceleration, velocity and displacement time histories of the forward-directivity Imperial Valley, El Centro Array #6 Station fault-normal record (left) and of the backward-directivity Landers, Joshua Tree Station fault-normal record (right). Note that the amplitude scales are different.

When assessing the vulnerability of stiff structures (i.e., a $T_1$ of 0.5s or shorter) like the woodframes considered here, however, rupture directivity effects are often neglected. The reason for doing so is two-fold. First, sites in the forward directivity region tend to experience larger than median fault-normal horizontal spectral quantities for a given magnitude and distance pair only at periods greater than 0.6s (Somerville *et al.*, 1997). Hence, for shorter period structures one may think that a customary approach to vulnerability assessment, which does not account explicitly for the special characteristics of near-source accelerograms, is appropriate. Second, the periods of the velocity pulses often found in forward-directivity, fault-normal horizontal components of ground motions are thought to be too much longer than the $T_1$ values of stiff structures to drive their nonlinear dynamic responses to unusually large demands.

In the development of analytical LFs, neglecting directivity effects translates into using: a) ground motions that are not necessarily near-source as input to the nonlinear dynamic analyses, and b) IMs as loss predictors that are not related to the pulse-like characteristics of the ground motion (e.g., pulse period) or to the location of the site with respect to the earthquake rupture (e.g., the directivity parameter Xcos(θ) or Ycos(ϕ) introduced by Somerville *et. al*., 1997). We will show below that this practice may lead to inaccurate descriptions of the vulnerability of some woodframe structures located close to faults and to inaccurate loss estimates for portfolios of such buildings.

## Ground Motions, Woodframe Structures, and Nonlinear Dynamic Analyses

To check whether two identical woodframe structures, one located in the forward and the other in the backward directivity region, are equally vulnerable to earthquake ground shaking of the *same severity*, we designed the following analytical exercise. We selected from the PEER Strong Ground Motion Database (http://peer.berkeley.edu/smcat/) 296 pairs of horizontal ground motion components extracted from over 40 earthquakes with moment magnitude ranging from 5.2 to 7.9 (including the 1979 Imperial Valley, 1989 Loma Prieta, the 1994 Northridge, the 1995 Kobe, and the 1999 Kocaeli, Duzce, and Chi-Chi Earthquakes). All of the ground motions (73 forward-directivity and 223 backward-directivity time-history pairs) were recorded within 20km of the ruptured fault on NEHRP $S_C$ to $S_E$ sites. The components were rotated to the fault-normal and fault-parallel directions (Abrahamson, 2005) prior to use. The range of spectral acceleration values, in terms of $S_a(T_1$=0.3s) for the woodframe structures considered in this study, is 0.08g to 3.0g for the forward-directivity subset and 0.04g to 4.13g for the backward-directivity subset. Stations that observed strong forward directivity conditions show values of the directivity parameter, Xcos(θ) for strike-slip faults and Ycos(ϕ) for dip slip faults, that are close to one, whereas sites in the neutral or backward directivity regions show values close to zero.

The results shown later were found using these 296 pairs of ground motions. However, to make sure that the imbalance in the number of forward- versus backward-directivity records did not color our results, we repeated the analyses using all available soil forward-directivity records within 50km of the fault rupture, as well as those recorded on NEHRP $S_A$ and $S_B$ sites. The results found using this augmented dataset, which consisted of 184 forward-directivity and 232 backward-directivity records, were very similar to those shown here and, therefore, support the results from the smaller set.

The 296 record pairs were used to establish the vulnerability of four types of woodframe houses that are common in the California residential building stock: $\mathbf{S_1}$, a small single-family dwelling, 1,200 ft$^2$ in area, 1-story in height, built around 1950, with an unbraced cripple wall and unbolted foundation; $\mathbf{S_2}$, like $S_1$ but with a slab-on-grade, bolted foundation; $\mathbf{L_1}$, a large single-family dwelling, 2,400 ft$^2$ in area, 2-stories high, built between 1940 and 1976, with an unbraced cripple wall and unbolted foundation; $\mathbf{L_2}$, a large single-family dwelling, 2,400 ft$^2$ in area, 2-stories high, built in the late 1980s to early 1990s and designed according to the 1988 Uniform Building Code

(ICBO, 1988), with a slab-on-grade, bolted foundation. These four woodframe buildings (see Fig. 2 for elevations) are variants of those considered in the CUREE-Caltech Woodframe Project (Isoda *et al*., 2001; Reitherman and Cobeen, 2003). The designs of the superstructures, with the exception of $L_1$, are the same as those developed by CUREE. The $L_1$ superstructure design, which is identical to $L_2$ except for the older vintage, was obtained by changing the characteristics of some shear walls in the $L_2$ design according to direction provided by Cobeen (2002).We modified the original foundation designs, when necessary, to model cripple walls and slab-on-grade foundations. The cost estimation work for replacing any damaged components of these houses is also taken from a CUREE report (Porter *et al.*, 2002). From Isoda *et al*. (2001) we also borrowed and modified, when necessary, the computer models of these houses for performing nonlinear dynamic analyses via RUAUMOKO (Carr, 2003).

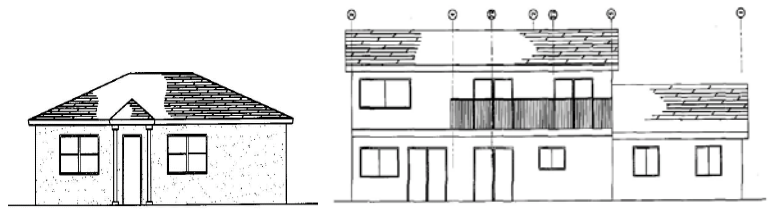

**Figure 2:** Elevation of the small dwelling, $S_1$ and $S_2$ (left) and of the large dwelling, $L_1$ and $L_2$ (right) taken from Isoda *et al*. (2001). The foundations below these elevations are explained in

The 296 pairs of recordings were used as input to nonlinear dynamic analyses to evaluate the response of these four buildings to different levels of ground shaking with both forward and backward directivity characteristics. The fault-parallel and fault-normal components of each pair were applied first in the East-West and North-South directions of the buildings, respectively, and then switched. Hence, in total, 592 nonlinear dynamic analyses were executed. Within each analysis we simulated: a) the dynamic response of the building whose severity was monitored in terms of drift ratios for each story and for the cripple wall, when one was present; b) the random damage state of each component given the building response severity; and c) the random repair cost for each component for a given damage state. As anticipated, following the CUREE methodology (Porter *et al.*, 2002), the total loss in each analysis was found by summing the repair or replacement costs for all damaged components. Note that the costs of fixing different components were treated independently with two significant exceptions: a) in the event of a failure of any cripple wall, the structure was considered to have collapsed and the entire cost of the structural repairs was treated as one random variable; b) the cost of painting damaged walls covers all the walls in the "line of sight", even if undamaged (Porter *et al*., 2002).

## Loss Functions for Woodframe Buildings

Summarized in Fig. 3 are results that show the trend of the mean loss ratio, *LR* (i.e., loss divided by building replacement cost) versus not only the 5%-damped $S_a$(0.3s), as more customarily done, but also the directivity parameter, *DP* (i.e., X$\cos(\theta)$ or Y$\cos(\phi)$). The surface is obtained via regression analysis with the following simple log-linear model:

$$\ln LR = a + b \ln S_a + c \ln DP + \varepsilon \sigma_{\ln LR} \qquad (1)$$

where $\varepsilon$ is a standard normal (Gaussian) random variable and $\sigma_{\ln LR}$ is the log standard deviation of *LR* for a given $S_a$(0.3s) and *DP*. Note that, consistent with the definition of spectral quantities adopted in most ground motion prediction equations, the values of $S_a$(0.3s) used in the regression are the geometric means of the spectral values of the two horizontal components. Also, the initial fundamental period of vibration of these woodframe buildings is close but shorter than the value of 0.3s selected here. We chose to use $S_a$(0.3s) for convenience because the United States Geological Survey customarily reports seismic hazard analysis results and earthquake scenario ShakeMaps at the a period of 0.3s (see http://earthquake.usgs.gov/hazmaps/ and http://www.trinet.org/shake/, respectively)

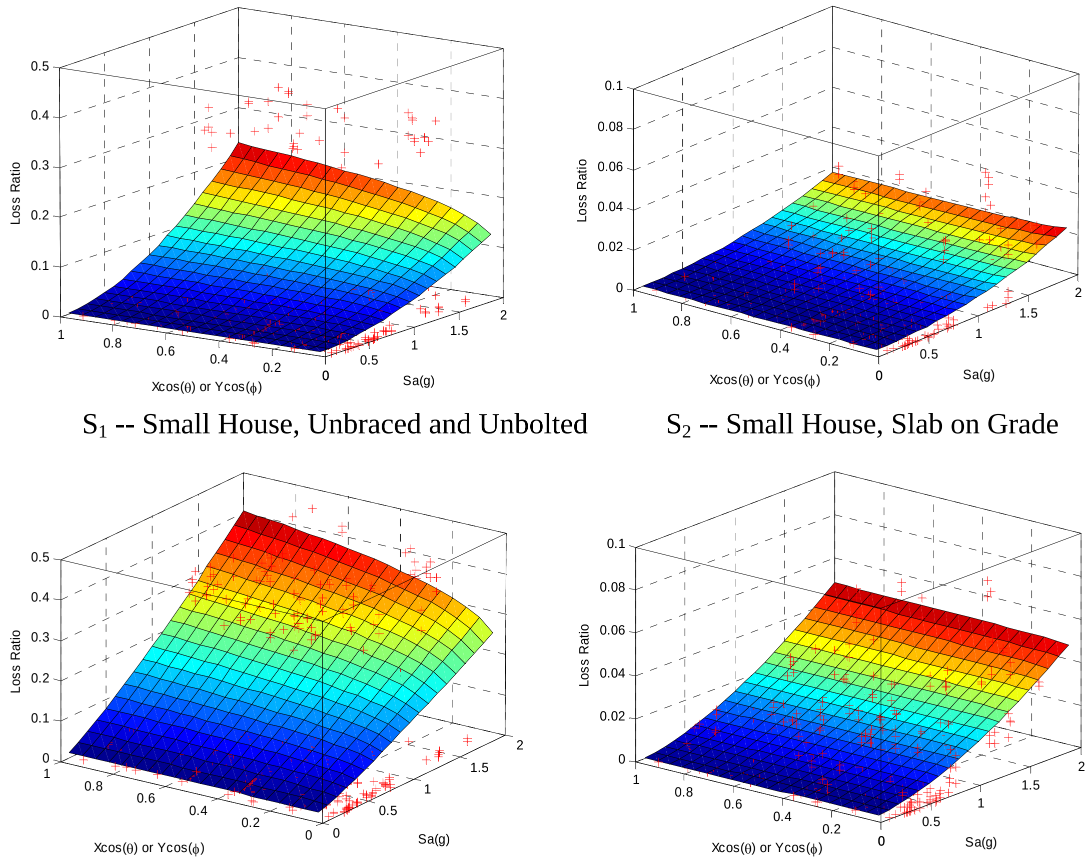


$S_1$ -- Small House, Unbraced and Unbolted

$S_2$ -- Small House, Slab on Grade

$L_1$ -- Large House, Unbraced and Unbolted

$L_2$ -- Large House, Slab on Grade

**Figure 3**: Loss functions for the four woodframe buildings considered in this study. Although not plotted here, the records with $S_a$(0.3s)>2.0g are used in the regression.

From Fig. 3 it is apparent that for $S_1$ and $L_1$ the median *LR* for a given $S_a$(0.3s) increases with increasing values of *DP*. This means that the characteristics of forward-directivity ground motions make them more aggressive than typical accelerograms with the same spectral ordinate, even for some of these woodframe buildings whose initial $T_1$ is much shorter than the period of the velocity pulses. As discussed more below, the pulse-like nature of fault-normal ground motion records in the forward directivity region tends to fail cripple walls more often than do neutral and backward-directivity records of the same severity. Also, the importance of *DP* is about the same for the two-story and the one-story buildings with slab-on-grade foundation, $S_1$ and $L_1$. The value of *c* in Eq. 1, which is 0.21 for $S_1$ and 0.17 for $L_1$, is statistically significantly different than zero at the 95% confidence level in both cases. For the $S_2$ and $L_2$ buildings with slab-on-grade foundations, *DP* does not appear to play an important role. The value of *c* is essentially zero in both cases (i.e., the mild departure from zero is not statistically significant at any customary confidence level) and $S_a$(0.3s) is the only informative predictor.

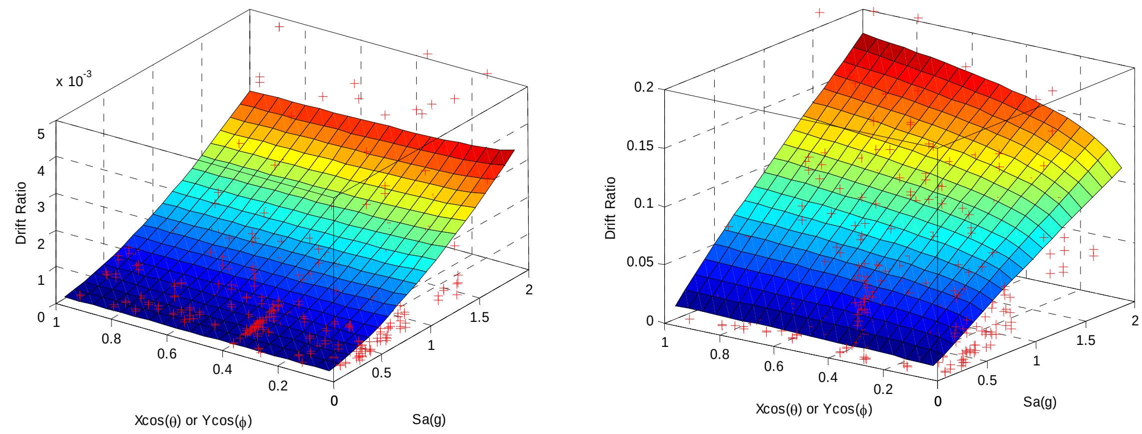


$S_2$ -- Small House, Slab on Grade    $L_1$ -- Large House, Unbraced and Unbolted

**Figure 4**: Drift ratio versus $S_a$(0.3s) and the directivity parameter for the $S_2$ and $L_1$ woodframe buildings. The drift for the $L_1$ case is computed at the top of the cripple wall (this drift ratio is larger than the roof drift ratio), whereas for the $S_2$ case it is computed at the roof level. Although not plotted here, the records with $S_a$(0.3s)>2.0g are used in the regression.

To understand the shape of the LFs in Fig. 3 it is useful to study the intermediate results in Fig. 4, which shows the maximum drift ratio across the two orthogonal horizontal directions versus the geometric mean $S_a$(0.3s) and the directivity parameter for the two extreme cases, $S_2$ (small house, slab on grade) and $L_1$ (large house, unbraced, unbolted). In both the $S_2$ and $L_2$ cases with slab-on-grade foundations, even very large accelerations do not, on average, cause the building to collapse (e.g., drift ratios of about 0.4% at 2g), thereby resulting in fairly small mean *LR*s (less than 10%). The negligible impact of *DP* may be partially explained by this limited level of nonlinearity in the buildings with slab-on-grade foundations. On the other hand, the two buildings with unbraced cripple walls and unbolted foundations, $S_1$ and $L_1$, tend to experience cripple-wall failure at large accelerations (e.g., drift ratios of about 18% at 2g). When the cripple walls fail the CUREE cost estimation methodology sets the median loss to only about 28% to 42% of the replacement cost under the assumption that the building can be jacked up and repaired rather than demolished and rebuilt.

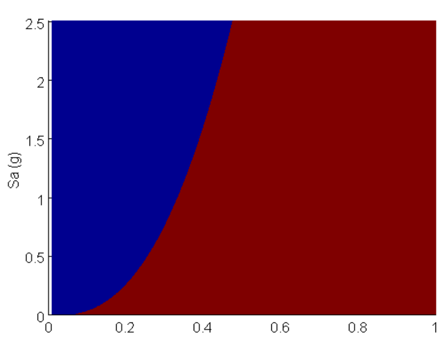


**Figure 5**: Neglecting directivity effects would result in systematically lower (higher) loss estimates for $L_1$ buildings within 20km of a rupture and for the $S_a$-*DP* pairs in the red (blue) region.

To summarize, if one were to neglect *DP* as a loss predictor and use only $S_a$(0.3s) for a $S_1$ or $L_1$ building close to a causative fault, then the resulting loss estimates could be inaccurate. Fig. 5 shows the regions of the $S_a$-*DP* domain in which using $S_a$(0.3s) as the only predictor would either overestimate (blue area) or underestimate (red area) the loss for an $L_1$ building. The accuracy of the total loss for a portfolio of $S_1$ and $L_1$ buildings estimated using only $S_a$(0.3s) will depend on the spatial distribution of the buildings with respect to each causative fault, as demonstrated in the next section.

## Results of Loss Estimation Analyses

To illustrate the use of the directivity-based LFs, we performed a series of test cases both on five specific single properties (yellow squares in Fig. 6), each considered separately, and on a portfolio of approximately 1,200 properties (blue dots in Fig. 6) located in the San Francisco Bay Area. The five sites are aligned with the Hayward Fault and located at 1km, 5km, 10km, 30km, and 50km from the S-E tip of the fault (i.e., where the directivity parameter defined by Somerville, *et al.* (1997) is maximized). Given the LF results described above, in these analyses we assumed that all of the structures were either $S_1$ or $L_1$, namely those sensitive to rupture directivity. We considered in total 5+1 exposures x 2 building types = 12 test cases. For each of the 12 test cases, we ran three sets of 10,000 simulations of a M7.0 event on the Rodgers Creek and Hayward Faults (the rupture is the green line in Fig. 6). In the three simulation sets the epicenter was either located: 1) near the N-W tip of the rupture; 2) near the S-E tip of the rupture; or 3) randomly located along the strike according to the bathtub-shaped probability distribution derived by Mai (2002). In each simulation set we randomly generated 10,000 $S_a(0.3s)$ values at each site using the Abrahamson and Silva (1997) ground motion prediction equation. In the portfolio analysis we kept the inter-event and the intra-event ground motion variability terms separated to produce correlated spectral acceleration random fields. The loss at each site was estimated using both the LF surfaces shown in Fig. 3 and those that neglect rupture directivity (not shown here).

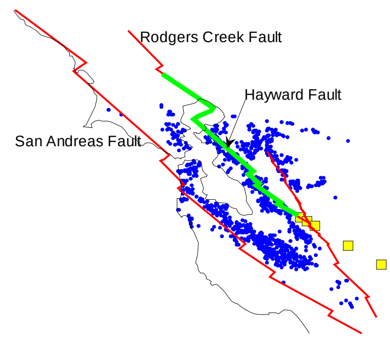


**Figure 6**: Portfolio (blue dots) and single properties (yellow squares) used in the loss estimation analyses. Also shown is the M7.0 rupture on the Rodgers Creek and Hayward Faults (green line).

**Table 1**: Loss statistics (in % of the replacement cost) for a single site located at 5km from the rupture (left panel) and for a portfolio (right panel) (see the map in Fig. 6). All the buildings are of type $L_1$.

| | Towards DP=0.87 | Away DP=0.05 | Random Epicenter | No Directivity |
|---|---|---|---|---|
| mean | 15.8 | 10.0 | 13.4 | 13.5 |
| median | 14.8 | 9.3 | 12.4 | 12.5 |

| | Towards | Away | Random Epicenter | No Directivity |
|---|---|---|---|---|
| mean | 10.3 | 8.1 | 9.0 | 9.4 |
| median | 9.6 | 7.6 | 8.3 | 8.8 |

The results of these test cases are shown in Tables 1 and 2. Table 1 reports the loss statistics for $L_1$ buildings located at the 5km site aligned with the fault (left panel) and at the portfolio of sites (right panel). As expected, the loss estimates for the rupture propagating in the S-E direction ("towards") are the highest not only for the single site but also for the portfolio. The latter is only true because this portfolio has more "mass" in the South Bay than in the North Bay. The lowest loss estimates are for the rupture propagating in the N-W direction ("away"). The increase in the mean losses from the forward (towards) to backward (away) directivity cases is about 58% for the single site and about 27% for the portfolio of sites. Neglecting rupture directivity altogether leads to mean loss estimates that are different by up to 35% in the single site case, and up to 16% in the portfolio case, from those that account for directivity. Note that the loss statistics in the random epicentral location case and those in the no directivity case are, however, within 5% of each other. It is emphasized that these differences between forward-directivity losses, backward-directivity losses and no-directivity losses are relatively small in this study because the amplitude of the IM that is correlated with the response of the stiff woodframe structures, namely $S_a(0.3s)$, is not affected by the direction of the rupture. The differences between the three cases are due solely to the effects of directivity on the LFs. The differences between losses for the directivity case with random epicenter (as well as those with constrained rupture direction) and losses for the no-directivity case would be more pronounced for more flexible structures ($T_1 > 0.6s$) that are additionally "hit" by the anisotropic distribution of ground motion in the near-source region.

In Table 2 the reader can find a concise summary of the maximum difference between the loss statistics computed by including or excluding directivity in the analyses performed on all five of the sites with both $L_1$ or $S_1$ woodframe building types.

**Table 2:** Maximum difference in the statistics of the loss estimates obtained by considering or neglecting directivity effects for $L_1$ or $S_1$ buildings located at any one of the five sites marked with yellow squares in Fig. 6.

| | Towards DP=0.87 | Away DP=0.05 | Random Epicenter |
|---|---|---|---|
| $L_1$ | 30% | -28% | 12% |
| $S_1$ | 50% | -36% | 17% |

The findings above can have a direct impact on Probable Maximum Loss (PML) studies that are routinely performed for insurance companies and financial lending institutions. PML studies often consider single scenario events, such as the M7.0 earthquake on the Hayward-Rodgers Creek Faults used here, but rarely explicitly include directivity in the ground motion and vulnerability (LF) calculation. As demonstrated above, the resulting inaccuracy in the loss estimates may be substantial.

Finally, note that the LFs derived in this study assumed fairly regular buildings, free of construction defects, located on flat ground. More realistic buildings, which often have complex floor plan configurations and roof geometries, imperfect construction and deferred maintenance, and which may be located on sloping sites, are likely to be more vulnerable to ground shaking than implied by these LFs. Hence, realistic losses that may occur to woodframe buildings such as those considered here are likely to be higher in a M7.0 Hayward event than those shown in Table 1. Calibration of the LFs with empirical loss data from past earthquakes can help to quantify this difference.

## Conclusions and Recommendations

In this study we showed that accounting for direction of rupture can be important when estimating the earthquake losses for some of the woodframe buildings that are commonly found in the California residential inventory. Using modifications of the models developed by the CUREE-Caltech Woodframe Project, we found, in particular, that accounting for directivity is important for the weaker and older buildings with unbraced cripple walls and unbolted foundations. Near-source, forward-directivity ground motions seem to cause cripple wall failures in such buildings more often than do typical backward-directivity and far-field accelerograms of the same severity. The pulse-like characteristics of fault-normal, forward-directivity ground motions is likely responsible for pushing the cripple walls to extremely high drift ratios. The effect of directivity on the vulnerability of the woodframe buildings with slab-on-grade foundations is, however, negligible. The effects of directivity on scenario loss estimates for structures with unbraced cripple walls located close to a causative fault can be significant whether the structures are considered individually or in a portfolio analysis. This study demonstrates that the loss estimates computed with and without directivity may, in extreme single cases, differ by as much as 50%. The differences for portfolio analyses are in general smaller and depend on the spatial distribution of the portfolio. If, however, an earthquake scenario with a unidirectional rupture and a narrowly-distributed portfolio is considered, the differences in the portfolio loss estimates with and without directivity effects may be substantial. These finding may have direct repercussions with respect to the accuracy of many PML calculations for portfolios of woodframe buildings that do not account for directivity. Finally, note that although we considered a specific earthquake scenario in this study, the concepts presented here will also have an impact on loss estimation analyses that use a probabilistically-based database of future earthquakes.

## References


Abrahamson, N.A., 2005. Personal Communication -- DVD containing PEER Rotated Records, San Francisco, CA, May.

Abrahamson, N.A., and W.J. Silva, 1997. Empirical Response Spectra Attenuation Relations for Shallow Crustal Earthquakes. *Seismological Research Letters*; **68**(1): 94-127.

Carr, A. J., 2003. RUAUMOKO – The Maori God of Volcanoes and Earthquakes, Computer Program Library, Department of Civil Engineering, University of Canterbury, New Zealand.

Cobeen, K., 2003. Personal Communication, Walnut Creek, CA, April.

International Conference of Building Officials (ICBO), 1988. *Uniform Building Code, Whittier*, CA

Isoda, H., Folz, B., and A. Filiatrault, 2001. Seismic Modeling of Index Woodframe Buildings. Report to CUREE No. SSRP-2001/12, Dept. of Structural Engineering, University of California, San Diego, La Jolla, CA.

Mai, P.M., 2002. Characterizing Earthquake Source Complexity for Improved Strong Motion Prediction, *Ph.D. Dissertation*, Department of Geophysics, Stanford University, Stanford, CA.

Porter *et al*., 2002. Improving Loss Estimation for Woodframe Buildings, The CUREE-Caltech Woodframe Project, CUREE Publication No. W-18, Richmond, CA.

Reitherman, R., and K. Cobeen, 2003. Design Documentation of Woodframe Project Index Buildings, The CUREE-Caltech Woodframe Project, CUREE Publication No. W-29, Richmond, CA.

Somerville, P.G., Smith, N.F., Graves, R.W., and N.A. Abrahamson, 1997. Modification of Empirical Strong Ground Motion Attenuation Relations to Include the Amplitude and Duration Effects of Rupture Directivity. *Seismological Research Letters*; **68**(1): 199-222.

Somerville, P.G., 2003. Magnitude Scaling of the Near Fault Rupture Directivity Pulse. *Physics of the Earth and Planetary Interiors*; **137**: 201-212.